Electronic Supplementary Material (ESI) for Nanoscale.

Cluster-size dependent internal dynamics and magnetic anisotropy of Ho ions in $HoM_2N@C_{80}$ and $Ho_2MN@C_{80}$ families (M = Sc, Lu, Y)

Y. Zhang,[a] D. Krylov,[a] S. Schiemenz,[a] M. Rosenkranz,[a] R. Westerström,[b,c] J. Dreiser,[c,d] T. Greber,[b] B. Büchner,[a] A. A. Popov[a]

Supporting Information

1. Synthesis and isolation of the $Ho_xY_{3-x}N@C_{80}$ and $Ho_xLu_{3-x}N@C_{80}$ (x= 1, 2)

Synthesis

Ho/Lu and Ho/Y MMNCFs were synthesized by the "selective organic solid" (SOS) route as described previously. Briefly, a mixture of Ho_2O_3, Y_2O_3 or Lu_2O_3 (99.9%, MaTeck GmbH, Germany), guanidine thiocyanate (GT) and graphite powder was used (molar ratio Ho/M/GT/C=1/1/2.5/15, M= Lu or Y). After dc-arc discharging, the soot was pre-extracted by acetone and further Soxhlet-extracted by CS_2 for 20h.

Isolation and Characterization

The isolation of Ho-based MMNCFs was performed by two-step HPLC. At the first step a linear combination of two analytical 4.6×250 mm Buckyprep columns (Nacalai Tesque, Japan) was applied on a Hewlett-Packard instrument (series 1100) with toluene as the eluent. Further isolation was performed by a recycling HPLC (Sunchrom, Germany) using a Buckyprep column (10×250 mm; Nacalai Tesque, Japan) and toluene as the eluent. The UV detector set to 320 nm was employed for fullerene detection for all steps. The details of HPLC isolation of Ho-based MMNCFs are described in the Supporting Information. The purity of the isolated products was checked by laser desorption/ionization time-of-flight (LDI-TOF) mass spectrometry (Biflex III, Bruker, Germany), the spectra are shown in supporting information as well. UV-Vis-NIR absorption spectra were measured in toluene solution using Shimadzu 3100 spectrometer.

1.1 Synthesis and isolation of $Ho_xY_{3-x}N@C_{80}$ (x=1, 2)

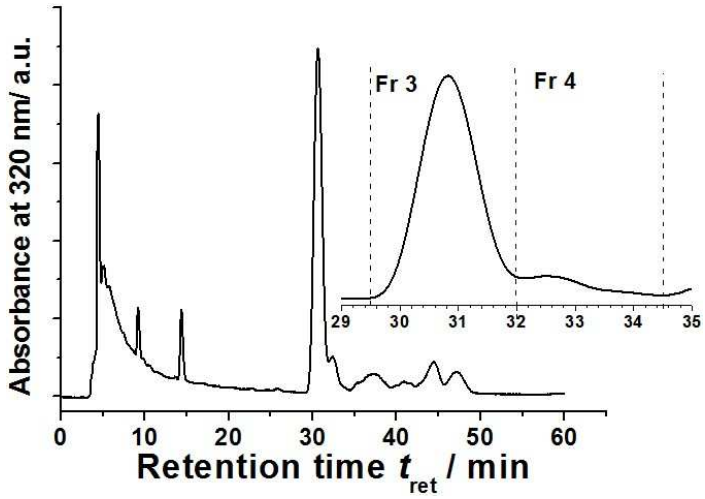

Figure S1. Chromatogram of a raw $Ho_xY_{3-x}N@C_{2n}$ fullerenes extract synthesized by the "selective organic solid" method (linear combination of two 4.6×250 mm Buckyprep columns, flow rate 1.6 ml/min, injection volume 200 μL, toluene as mobile phase, 40 ℃). The inset shows the enlarged chromatographic region of 29.5-34.5 min.

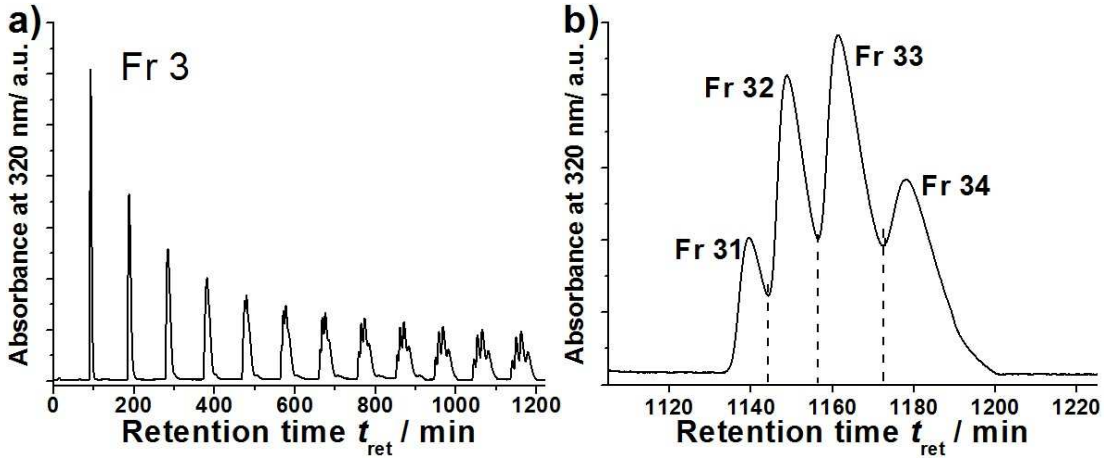

Figure S2. The HPLC isolation of fraction Fr 3. (10×250 mm Buckyprep column; flow rate 1.5 ml/min; injection volume 5 ml; toluene as eluent; 20 ℃).

The synthesis of $Ho_xY_{3-x}N@C_{80}$ (x= 1, 2) was achieved by "selective organic solid" route. The process of dc-arc discharging and solution extraction was the same in the production of $Ho_xSc_{3-x}N@C_{80}$ (I; x=1, 2). A mixture of Ho_2O_3 and Y_2O_3 (99.9%, MaTeck GmbH, Germany), guanidine thiocyanate (GT) and graphite powder was used (molar ratio Ho/Y/GT/C=1:1:2.5:15). The chromatogram of the extracted $Ho_xY_{3-x}N@C_{2n}$ fullerenes is shown in Figure S1. The $Ho_xY_{3-x}N@C_{80}$ (I, x= 1, 2) were isolated by multistep HPLC (see Figure S2-5). Firstly, the analytical HPLC was employed to collect $Ho_xY_{3-x}N@C_{80}$ (I) (Fraction 3) and $Ho_xY_{3-x}N@C_{80}$ (II) (Fraction 4) respectively. Different to $Ho_xSc_{3-x}N@C_{80}$ (I, x= 1, 2), the retention time of $Ho_xY_{3-x}N@C_{80}$ (I) in Buckyprep column (4.6×250 mm) are identical. Secondly, the Fr 3 was subjected to isolation by recycling HPLC on a Buckyprep column (10×250 mm), see Figure S2. After 12 cycles, four sub-fractions could be obtained which marked as Fr 31 to Fr 34. The relative yield of $Ho_xY_{3-x}N@C_{80}$ (x= 0-3) could be estimated from the integrated areas of the corresponding chromatographic peaks which agrees well with mass spectrum result of Fr 3 (Figure S 2b).

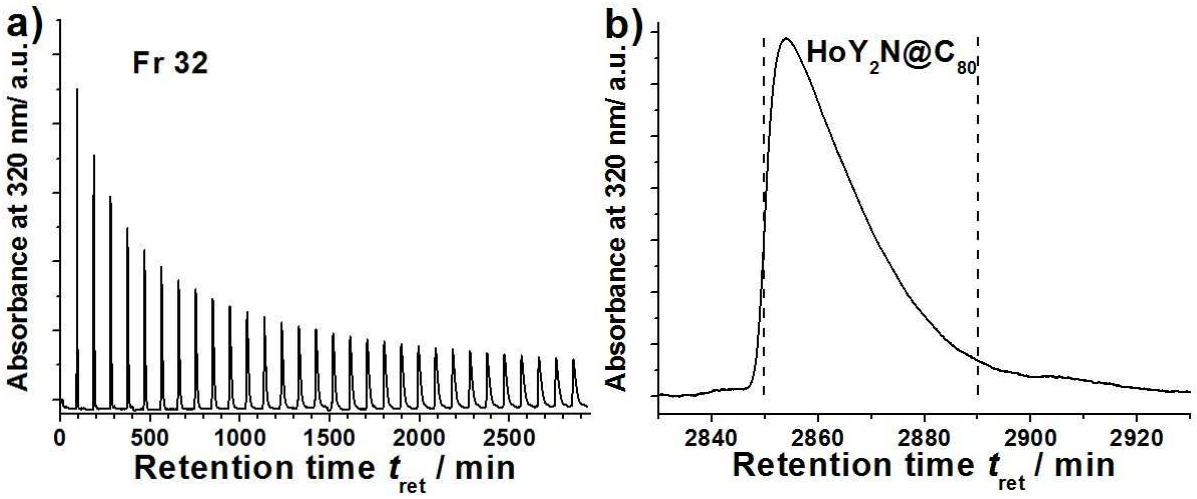

Figure S3. The isolation of fraction Fr 32. (10×250 mm Buckyprep column; flow rate 1.5 ml/min; injection volume 5 ml; toluene as eluent; 20 ℃).

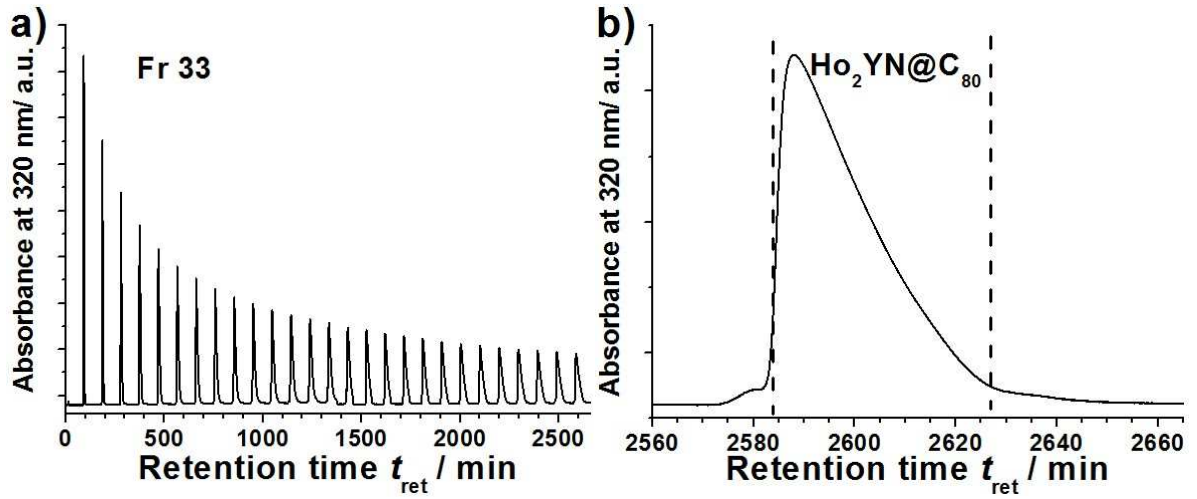

Figure S4. The isolation of fraction Fr 33. (10×250 mm Buckyprep column; flow rate 1.5 ml/min; injection volume 5 ml; toluene as eluent; 20 ℃).

Isolation of $HoY_2N@C_{80}$ (I) was accomplished by removing the small amount of $Y_3N@C_{80}$ (I) and $Ho_2YN@C_{80}$ (I) from fraction 32 after 30 cycles. Similarly, the pure $Ho_2YN@C_{80}$ (I) could be obtained by removing the minor structures ($HoY_2N@C_{80}$ (I) and $Ho_3N@C_{80}$ (I)) in fraction 33 through 27 cycles. The purity of $Ho_xY_{3-x}N@C_{80}$ (I, x= 1, 2) were confirmed by LDI-TOF mass spectroscopy (Figure S5).

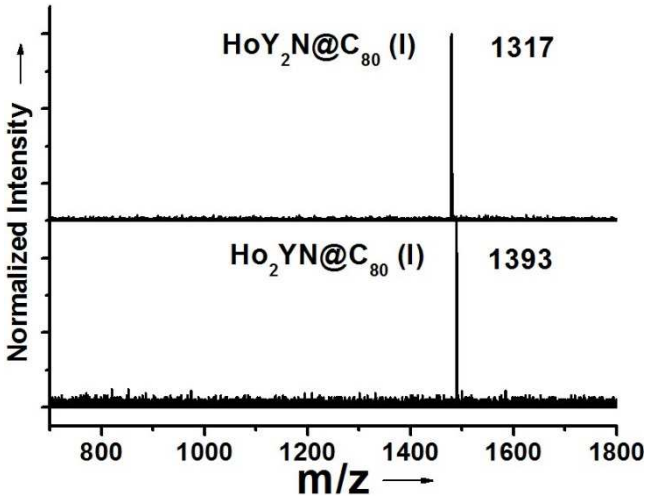

Figure S5. The isolated samples of $Ho_xY_{3-x}N@C_{80}$ (I; x= 1, 2) were identified by laser-desorption/ionization time-of-flight (LDI-TOF) mass spectrum analysis, which confirmed their high purity.

1.2 Synthesis and isolation of $Ho_xLu_{3-x}N@C_{80}$ (I, x=1, 2)

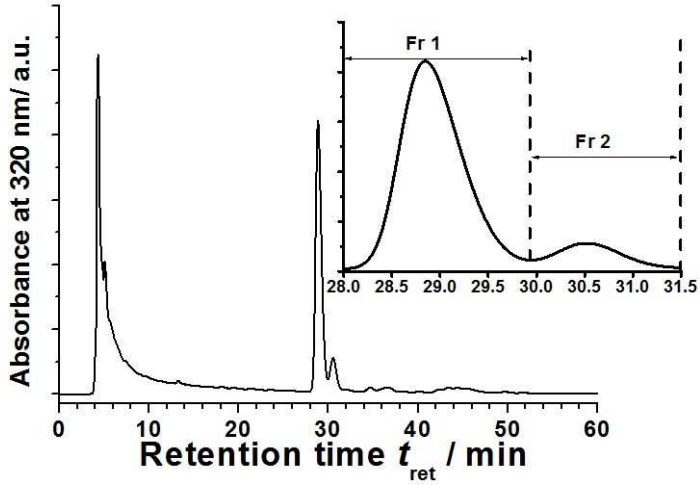

Figure S6. Chromatogram of a raw $Ho_xLu_{3-x}N@C_{2n}$ fullerenes extract synthesized by the "selective organic solid" method (linear combination of two 4.6×250 mm Buckyprep columns, flow rate 1.6 ml/min, injection volume 200 μL, toluene as mobile phase, 40 ℃). The inset shows the enlarged chromatographic region of 28.0-31.5 min.

The synthesis of $Ho_xLu_{3-x}N@C_{80}$ (x= 1, 2) was achieved by "selective organic solid" route as). A mixture of Ho_2O_3 and Lu_2O_3 (99.9%, MaTeck GmbH, Germany), guanidine thiocyanate (GT) and graphite powder was used (molar ratio Ho/Lu/GT/C=1:1:2.5:15).

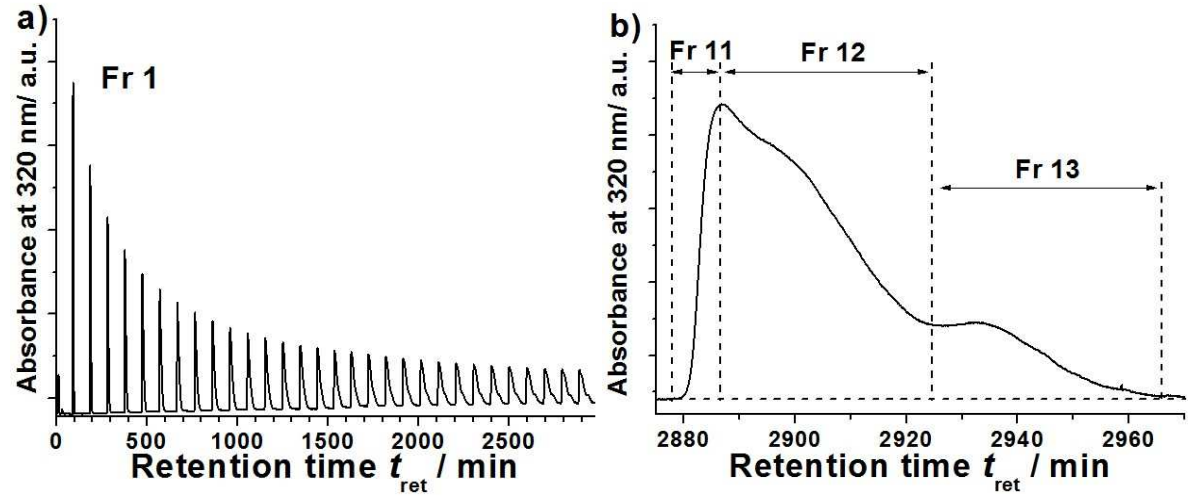

Figure S7. The isolation of fraction Fr 1. (10×250 mm Buckyprep column; flow rate 1.5 ml/min; injection volume 5 ml; toluene as eluent; 20 ℃).

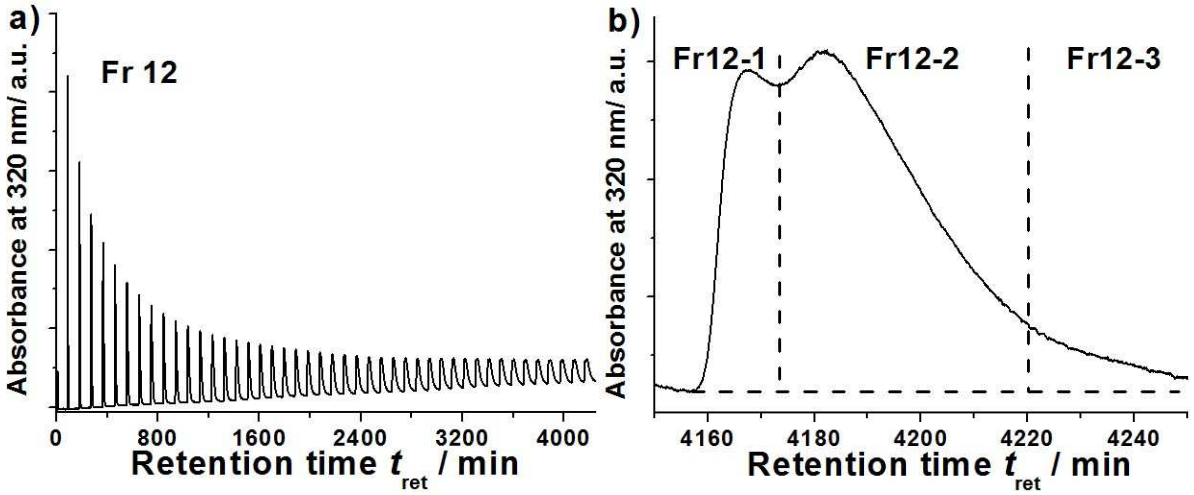

Figure S8. The isolation of fraction Fr 12. (10×250 mm Buckyprep column; flow rate 1.5 ml/min; injection volume 5 ml; toluene as eluent; 20 ℃).

The mixture of $Ho_xLu_{3-x}N@C_{2n}$ was subjected to isolation by analytical HPLC in the first step (Figure S6). $Ho_xLu_{3-x}N@C_{80}$ (I) and $Ho_xLu_{3-x}N@C_{80}$ (II) were separated into Fr 1 (28.0-29.9 min) and Fr 2 (29.9-31.5 min) respectively according to the difference of their cage symmetry. In the second step, three sub-fractions could be obtained after recycling fraction 1 over 30 times which then named as Fr 11, Fr 12 and Fr 13. Checking by mass spectrum, the dominant structure in Fr 12 is $Ho_xLu_{3-x}N@C_{80}$ (I) (Figure S7). In the third step, the Fr 12 was subjected to recycling HPLC again for removing minor structures ($HoLu_2N@C_{80}$ (I) and $Ho_3N@C_{80}$ (I)). As shown in Figure S8, Fr 122 was collected after 44 cycles. In the fourth step, after running another 44 cycles, the isolation of $Ho_2LuN@C_{80}$ (I) was successfully achieved and its purity was confirmed by LDI-TOF mass spectroscopy (Figure S11).

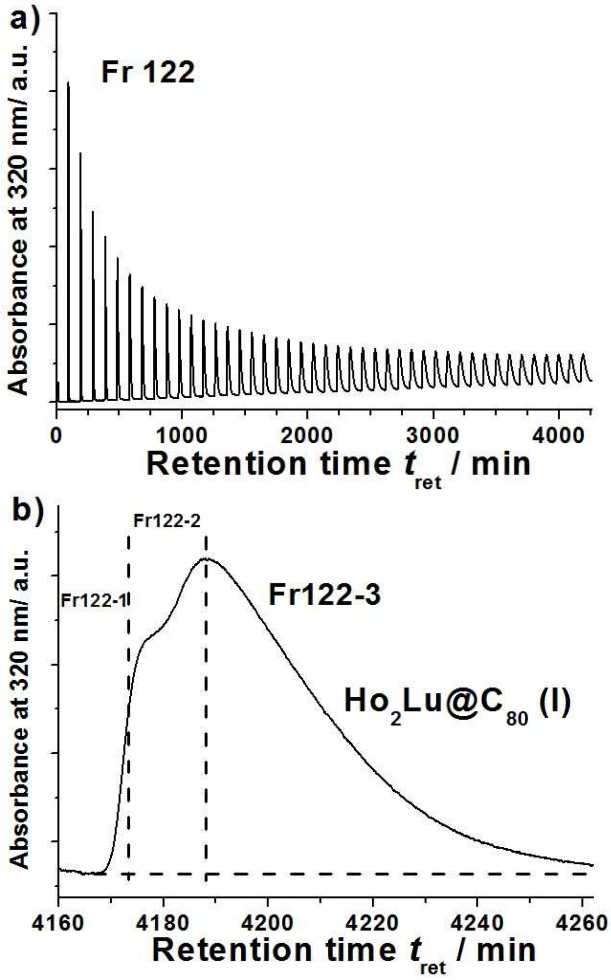

Figure S9. The isolation of fraction Fr 122. (10×250 mm Buckyprep column; flow rate 1.5 ml/min; injection volume 5 ml; toluene as eluent; 20 ℃).

Similar to $Ho_2LuN@C_{80}$ (I), the isolation of $HoLu_2N@C_{80}$ (I) is extremely time-consuming due to the retention time of $Lu_3N@C_{80}$ (I) and $HoLu_2N@C_{80}$ (I) is almost identical. Only by running on recycling HPLC over 73 cycles, small amount of $HoLu_2N@C_{80}$ (I) could be obtained, see Figure S10. The purity of $HoLu_2N@C_{80}$ (I) was confirmed by LDI-TOF mass spectroscopy (Figure S11).

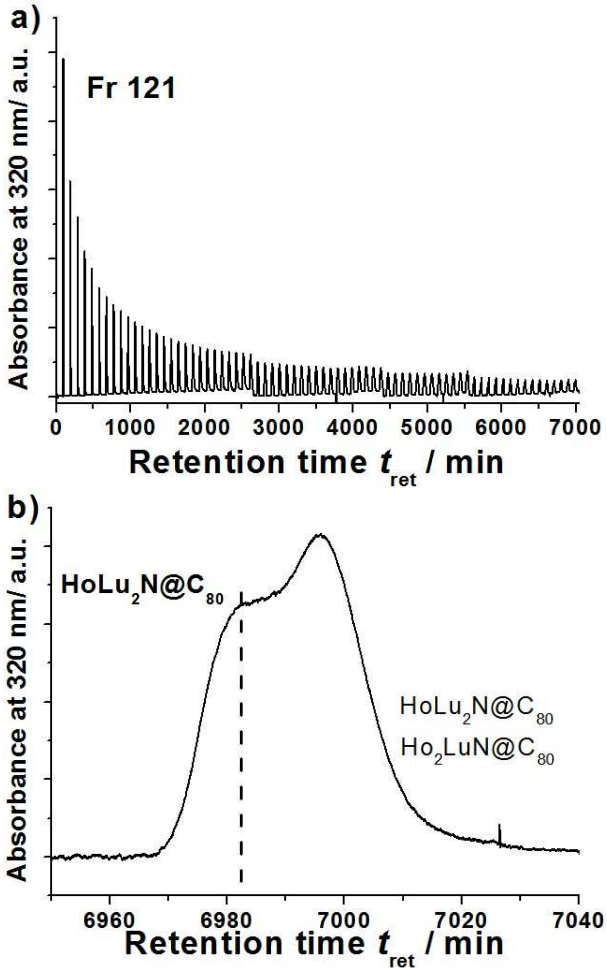

Figure S10. The isolation of fraction Fr 121. (10×250 mm Buckyprep column; flow rate 1.5 ml/min; injection volume 5 ml; toluene as eluent; 20 ℃).

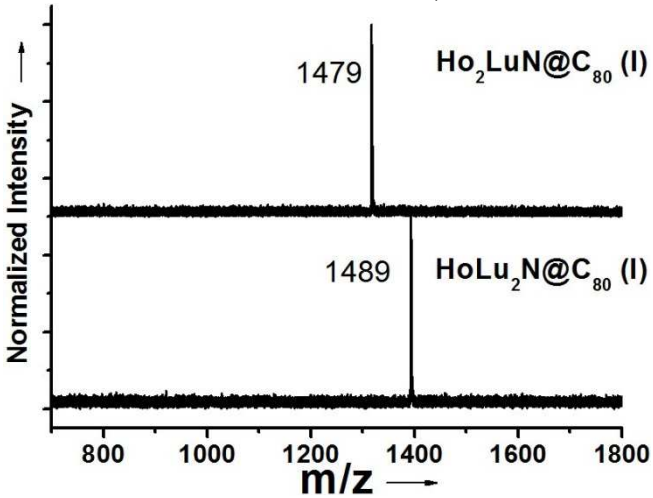

Figure S11. The isolated samples of $Ho_xLu_{3-x}N@C_{80}$ (I; x= 1, 2) were identified by LDI-TOF mass spectrum analysis, which confirmed their high purity.

2. Spectroscopic properties of $Ho_xM_{3-x}N@C_{80}$ (I; M= Y and Lu; *x*=1, 2)

2.1 UV-vis-NIR spectra of $Ho_xM_{3-x}N@C_{80}$

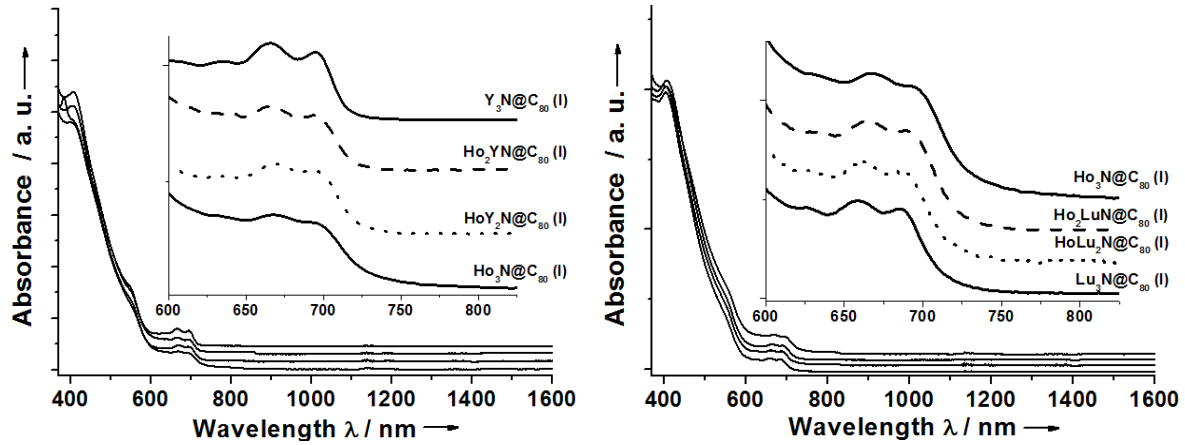

Figure S12. UV-vis-NIR spectra of $Ho_xY_{3-x}N@C_{80}$ (I; *x*= 0–3) (left) and $Ho_xLu_{3-x}N@C_{80}$ (I; *x*= 0–3) (right) in toluene.

2.2 FTIR spectra of $Ho_xM_{3-x}N@C_{80}$ (I; *x*=0–3)

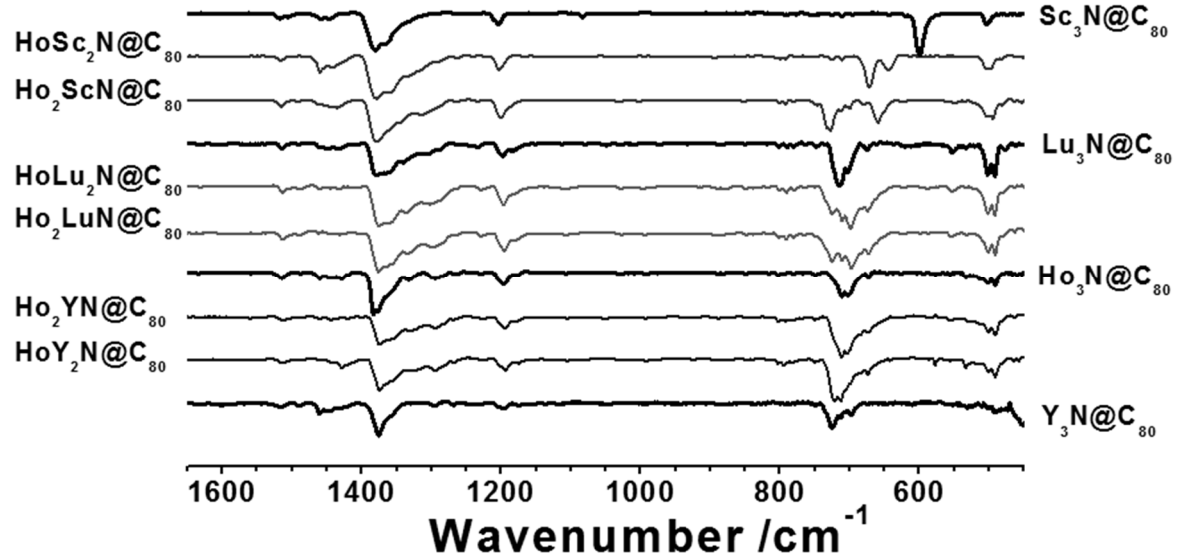

Figure S13. FTIR spectra of $Ho_xM_{3-x}N@C_{80}$ (I; M= Y, Lu; *x*= 0–3) compared with $Ho_xSc_{3-x}N@C_{80}$.

3. Quantum chemical calculations

B3LYP calculations were performed using the Firefly code.[1] The basis set was def2-SVP[2] for carbon atoms, def2-TZVP[2] for nitrogen, Stuttgart-Cologne effective core potentials for Sc (ECP10MDF)[3] with {3,1,1,1,1,1/2,2,1,1/4,1,1/1,1/1} valence part, ECP28MWB[4, 5] for Y with {3,1,1,1,1/4,1,1/4,1/1} valence electron part, and 4f-in-core ECP56MWB-II for Ho with {3,1,1,1,1,1/3,1,1,1,1/2,1,1,1,1/1,1,1/1,1} valence part.[6]
For QTAIM calculations, computations were performed using ORCA,[7] PBE functional, DKH relativistic correction, and DKH-TZVP full electron basis set.[8]

1. A. A. Granovsky, 2013. Firefly version 8.0.0, http://classic.chem.msu.su/gran/firefly/index.html
2. F. Weigend and R. Ahlrichs, *Phys. Chem. Chem. Phys.*, 2005, **7**, 3297-3305.
3. M. Dolg, U. Wedig, H. Stoll and H. Preuss, *J. Chem. Phys.*, 1987, **86**, 866-872.
4. D. Andrae, U. Häußermann, M. Dolg, H. Stoll and H. Preuß, *Theor. Chim. Acta*, 1990, **77**, 123-141.
5. X. Cao and M. Dolg, *J. Chem. Phys.*, 2001, **115**, 7348-7355.
6. M. Dolg, H. Stoll, A. Savin and H. Preuss, *Theor. Chim. Acta*, 1989, **75**, 173-194.
7. F. Neese, *WIREs Comput. Mol. Sci.*, 2012, **2**, 73-78.
8. D. A. Pantazis, X.-Y. Chen, C. R. Landis and F. Neese, *J. Chem. Theory Comput.*, 2008, **4**, 908-919.

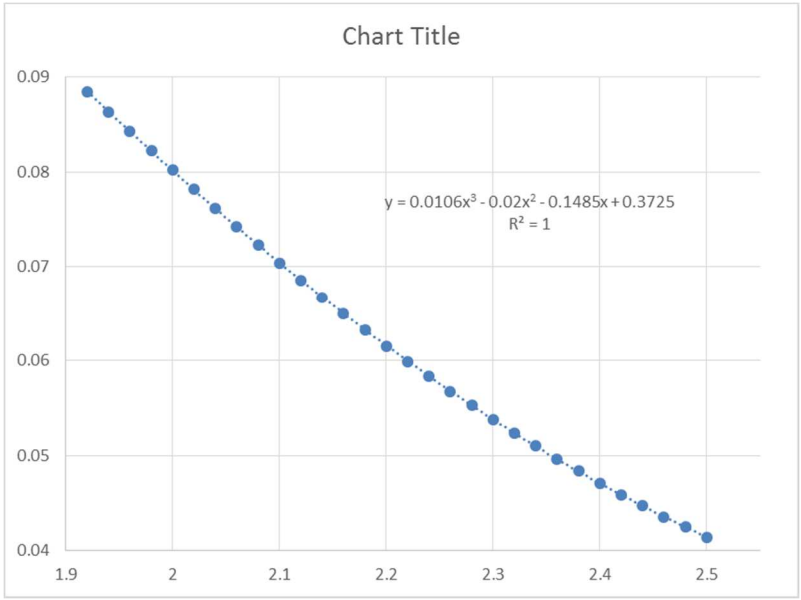

Correlation between $\Delta\chi$ (arb. unts) and Ho-Sc distance. The fitted polynomial was used to compute $\Delta\chi$ at any point of the MD trajectory.